



Original Article

Modelling growth and reproduction of Antarctic krill, *Euphausia superba*, based on temperature, food and resource allocation amongst life history functions

Andrew John Constable^{1,2,*} and So Kawaguchi^{1,2}

¹Australian Antarctic Division, Department of the Environment and Energy, 203 Channel Highway, Kingston, Tasmania 7050, Australia

²Antarctic Climate and Ecosystems Cooperative Research Centre, University of Tasmania, Private Bag 80, Hobart, Tasmania 7001, Australia

*Corresponding author: tel: +61 3 6232 3558; fax: +61 3 6232 3351; e-mail: andrew.constable@aad.gov.au.

Constable, A. J. and Kawaguchi, S. Modelling growth and reproduction of Antarctic krill, *Euphausia superba*, based on temperature, food and resource allocation amongst life history functions. – ICES Journal of Marine Science, 75: 738–750.

Received 10 May 2017; revised 14 September 2017; accepted 18 September 2017; advance access publication 20 October 2017.

Estimates of productivity of Antarctic krill, *Euphausia superba*, are dependent on accurate models of growth and reproduction. Incorrect growth models, specifically those giving unrealistically high production, could lead to over-exploitation of the krill population if those models are used in setting catch limits. Here we review available approaches to modelling productivity and note that existing models do not account for the interactions between growth and reproduction and variable environmental conditions. We develop a new energetics moult-cycle (EMC) model which combines energetics and the constraints on growth of the moult-cycle. This model flexibly accounts for regional, inter- and intra-annual variation in temperature, food supply, and day length. The EMC model provides results consistent with the general expectations for krill growth in length and mass, including having thin krill, as well as providing insights into the effects that increasing temperature may have on growth and reproduction. We recommend that this new model be incorporated into assessments of catch limits for Antarctic krill.

Keywords: Antarctica, CCAMLR, growth, krill, life history, modelling.

Introduction

Antarctic krill, *Euphausia superba*, (hereafter “krill”) is a keystone prey species of the Antarctic marine ecosystem. Its productivity is central to the success of the ecosystem but its prognosis is not well understood (Nymand-Larson *et al.*, 2014); recent studies suggest a vulnerability to the effects of climate change (Murphy *et al.*, 2017). Krill are also the target of the largest fishery, by mass, in the Southern Ocean and could become one of the largest fisheries in the world if the catch limits become fully exploited (Nicol *et al.*, 2012). The abundance of krill varies regionally (Nicol *et al.*, 2000), has great inter-annual variability, and has been postulated to be declining (Constable *et al.*, 2014). This variability and change could have consequent impacts on krill predators and the magnitude of ecologically sustainable catch limits for the krill fishery (Constable *et al.*, 2000, Constable, 2011, Nymand-Larson *et al.*, 2014, Constable *et al.*, 2014). The ecological

sustainability of catch limits is dependent on the variability and magnitude of the productivity of krill, along with the requirements for predators (Constable and de la Mare, 1996). Here, we focus on methods for evaluating and modelling the productivity of krill.

The earliest models of krill growth assumed that krill mature and reproduce once in their lifetime; length frequency distributions (LFDs) typically show two modes, giving the appearance of a 2-year life span (e.g. Rudd, 1932). Fifty years later, the current view was established that krill are likely to live for 5–6 years, growing to a maximum of ~60 mm (Aseev, 1984; Ikeda *et al.*, 1985).

For krill stock assessments, productivity is currently fixed through a seasonally adjusted, von Bertalanffy (vB) length-at-age function, and reproduction modelled using a mean and variability of recruitment (Constable and de la Mare, 1996). Although this may have been suitable for setting catch limits in the early

phase of the krill fishery, it is likely to be no longer appropriate given the long-term and regionally-specific changes occurring in the Antarctic marine ecosystem (Constable *et al.*, 2014). Hill *et al.* (2013) used outputs from an Earth-system model to explore how krill growth might respond to change in ocean temperatures in the South Atlantic under emission scenarios from the Intergovernmental Panel on Climate Change (IPCC). They applied the temperature-sensitive krill growth model of Atkinson *et al.* (2006, 2008) to spatially-resolved time series of temperature and determined change in the location and abundance of krill habitat that yields positive growth in length. However this model is not designed to address the effects of climate change on physiology, energetics, and fecundity of krill, which are the primary factors governing productivity.

Over the last decade, the interaction between food, temperature and the moult cycle is being shown to be important in determining growth and reproduction in Antarctic krill (Kawaguchi *et al.*, 2007b; Wiedenmann *et al.*, 2008, Brown *et al.*, 2010). A great challenge for establishing realistic models of growth and reproduction is to reconcile different limiting processes in krill and their interactions, including the exoskeleton, the body and gonadal masses, and the seasonal cycle in the physiology of krill (Kawaguchi *et al.*, 2007b; Meyer and Teschke, 2016). The moult cycle of krill imposes physical limits to rates of shrinkage and growth in length. Krill can gain and lose weight within its exoskeleton, through the deposition of lipids and gonads, which, in turn, can be used as storage to meet the requirements of metabolism in periods of starvation. Last, the extreme seasonality of the polar environment, particularly day length, means that reproduction is not only dependent on food supply but also on whether the gonads are active after a period of winter regression. At present, available models do not fully account for these factors.

In this article, we first review current approaches to model growth and reproduction in krill. We then develop a coupled energetics and moult-cycle (EMC) model sensitive to variability in food and temperature. The EMC model combines energetics, including the potential for reproduction to compete for resources with growth, and empirical data on the moult-cycle, growth rates and reproductive output. Last, we discuss the implications of this new model, which aims to facilitate easier adaptation of production models to changing environments, regionally and over years, as well as providing a balanced carbon model in order to be able to investigate the role of krill in the carbon cycle.

Review of models of krill productivity

vB growth

vB growth models [Table 1, Equation (1.1); Figure 1] (see review by Siegel and Nicol 2000) are a widespread class of growth models for Antarctic krill. Rosenberg *et al.* (1986) applied the first vB model to krill from 8 years (1928–1938) of data from the Discovery expeditions; growth rates were consistently high and modulated with a strong seasonal pattern. These patterns were described by a seasonally punctuated vB (PvB) model, concluding krill take 6–7 years to reach 60 mm which is the upper range of their size [Table 1, Equation (1.2); Figure 1]. Siegel (1987) discriminated the size of age classes from LFDs from different seasons and locations of the Antarctic Peninsula area. He fitted a vB model to a 5–6 year life span for krill. He further used a modified vB equation which considers seasonal growth oscillations (SvB) [Table 1, Equation (1.3); Figure 1].

Growth based on moult cycles

Following the model formulation of Wiedenmann *et al.* (2008), the class of growth models based on the moult cycle has no growth in length during the intermoult period (IMP) and then adding a growth increment at the time of moulting [Table 1, Equation (1.4)]. This model allows exploration of growth under different environmental conditions (seasonally and spatially varying food and temperature).

A meta-analysis of published data, using log-linear regression, has shown the IMP of krill is significantly related to sea-surface temperature, T [Table 1, Equation (1.5)] (Kawaguchi *et al.*, 2006). Without considering the effects of food on growth rates, this relationship creates a seasonal cycle in mean daily growth rates with slower growth in winter compared with summer. Tarling *et al.* (2006) report a binary logistic regression model relating IMP in summer to temperature, body length and sex/maturity stage; food was not a significant factor. Broader application of this model will need observations from other areas and seasons.

Instantaneous growth rates (IGRs) enable empirical models of growth in length of krill, dL ; they vary with sex, length, season and region. IGR is a method for measuring the change in size of living krill at the time of moulting (Quetin and Ross, 1991; see Kawaguchi *et al.*, 2006 for review). Crustaceans grow or shrink in size as they moult (Hartnoll, 2001). The length of a discarded moult represents the length of animals before the moulting event. The growth increment at the time of moult is, therefore, the length of animal after moult less the length of a discarded moult. IGR is defined as the growth increment expressed as a proportion of pre-moult total length but is often reported in units of length. In turn, daily growth rates are the IGR divided by the IMP (Kawaguchi *et al.*, 2006). These measurements can then be related to ambient environmental conditions during the previous IMP (Ross *et al.*, 2000).

Candy and Kawaguchi (2006) and Kawaguchi *et al.* (2006) model IGR using a Linear Mixed Model with 10 years of IGR measurements covering most of the growing season (November to April). The seasonal factor in IGR is a mixed effect factor in this model, incorporating both seasonal and food effects. The results provide a general indication of seasonal trends but are difficult to use as a means of determining change in IGR with food supply. Candy and Kawaguchi (2006) examined how the modified vB models (PvB and SvB) trace the actual growth pattern measured through their IGR experiments. They showed that neither the seasonal PvB model nor the seasonal oscillated SvB model can trace the rapid seasonal growth derived from those experiments. Instead they used a simple empirical model based on the cumulative F-distribution [Table 1, Equation (1.6); Figure 1]

Atkinson *et al.* (2006) also used an IGR model to estimate instantaneous krill growth given temperature and the concentration of food, both of which were measured in the field locations where the IGR experiments were undertaken. In their study the IGR experiments were undertaken during mid-summer (January and February) over two consecutive years (2002 and 2003). The authors noted that this model is difficult to apply outside of the summer experimental conditions because it does not fully account for the interaction between food, temperature and growth. Wiedenmann *et al.* (2008) used this IGR model combined with the IMP model of Kawaguchi *et al.* (2006). They attempted to use satellite Chlorophyll a data as surrogates for food concentration

Table 1. Historical models of productivity in Antarctic krill. Growth curves are illustrated in Figure 1.

Title	No.	Equation	Parameters and values	References
vB growth	1.1	$L_t = L_\infty (1 - e^{-K(t-t_0)})$	t age L_t Length at time t L_∞ length at infinity K IGR t_0 offset to give the finite length at $t = 0$ $L_\infty = 60$ mm; $K = 0.45$; $t_0 = 0.0$	Reviewed by Siegel and Nicol (2000) Parameters from Rosenberg <i>et al.</i> (1986)
PvB growth	1.2	$L_t = \begin{cases} L_\infty \left(1 - e^{-\frac{K}{g}(t-A(1-g))} \right) & A < t \leq (A+g) \\ L_\infty (1 - e^{-K(A+1)}) & (A+g) < t \leq (A+1) \end{cases}$	Symbols as in Equation (1). A age in years as winters survived g prop. of year in which growth occurs, starting at beginning of year $L_\infty = 60$ mm; $K = 0.45$; $t_0 = 0.0$; $g = 0.25$	Rosenberg <i>et al.</i> (1986)
SvB growth	1.3	$L_t = L_\infty \left(1 - e^{-\left[K(t-t_0) + \frac{\theta_0 K}{2\pi} \sin [2\pi(t-\theta_1)] \right]} \right)$	Symbols as in Equation (1). θ_0, θ_1 constants $L_\infty = 61$ mm; $K = 0.4728$; $t_0 = 0.1418$; $\theta_0 = 0.9598$; $\theta_1 = 0.0272$	Siegel (1987)
Moult-cycle IGRs	1.4	$L_t = \int_{t'=0}^t dL_{t'} \delta_{t'} dt \quad \begin{cases} \delta_{t'} = 1 & \text{if } IMP_{t'} = \text{int}(IMP_{t'}) \\ \delta_{t'} = 0 & \text{otherwise} \end{cases}$	dL growth increment (mm) $\delta t'$ whether a moult has just occurred following an IMP $IMP_{t'}$ number of IMPs up to that time including partial IMPs.	after Wiedenmann <i>et al.</i> (2008)
IMP	1.5	$IMP = \exp [\alpha_0 + \alpha_1 \ln (T + 2)]$	T temperature (°Celsius) α_0, α_1 constants. $\alpha_0 = 3.5371$; $\alpha_1 = 0.5358$	Kawaguchi <i>et al.</i> , 2006
Kawaguchi and Candy IGR growth	1.6	$L_t = \begin{cases} L_A + F'(L_{A+1} - L_A) & 1 < A < (t+g_0) \leq (A+g_1) \\ L_{A+1} & (A+g_1) < (t+g_0) \leq (A+1), A > 1 \end{cases}$ and $F' = F_{50,50} \left(2\beta \frac{(t+g_0-A)}{g_1} \right)$	A age in years as winters survived $F_{50,50}$ cum. prob. F-distribution, with 50 deg. of freedom for num. and denom. β constant g_0 prop. year from nominated birthday, say 1 Dec., to start of growing year g_1 prop of year in which growth occurs $L_2 = 28.0, L_3 = 41.77, L_4 = 48.95, L_5 = 53.55,$ $L_6 = 57.53, L_7 = 61.06$ $\beta = 1.239, g_0 = 0.8329$ year, $g_1 = 0.5808$ year $\beta_0 = 6.60, \beta_1 = -0.385,$ $\beta_2 = 0.00259,$ $\beta_3 = 17.53, \beta_4 = 0.332,$ $\beta_5 = 0.595, \beta_6 = -0.477$	Candy and Kawaguchi (2006)
Atkinson IGR growth	1.7	$dL(t) = \beta_0 + \beta_1 L(t) + \beta_2 L(t)^2 + \frac{\beta_3 f(t)}{\beta_4 + f(t)} + \beta_5 T(t) + \beta_6 T(t)^2$	T Temperature (°C) at time t $f(t)$ concentration of food at time t	Atkinson <i>et al.</i> (2006)

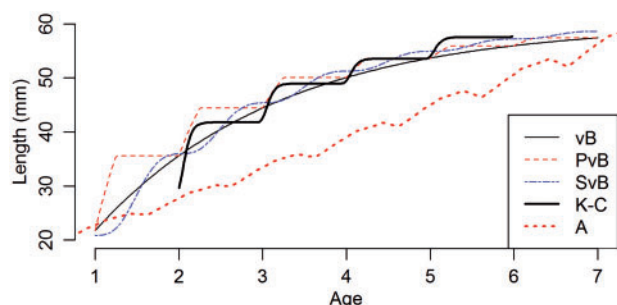


Figure 1. Length (mm) versus age (years) for different historical growth models for Antarctic krill, as detailed in Table 1. Different lines represent: vB (thin solid) and PvB (thin dash) of Rosenberg *et al.* (1986); SvB (thin solid wave) of Siegel (1987); moult-cycle models of Candy and Kawaguchi (2006) (KC, thick solid) and Atkinson *et al.* (2006) (A, thick dash).

but could not obtain growth trajectories that replicated observations. We corrected length in the equation to metre units and found the trajectories comparable with other models when using the Chlorophyll *a* time series described below [Table 1, Equation (1.7); Figure 1].

IGR models have not yet accounted for the density of krill when estimating the respective parameters. IGR is a function of the amount of food consumed, which in turn is affected by spatial and seasonal variation in food availability combined with density of krill and feeding efficiency under different conditions. Ideally, these factors will need to be considered in future development of IGR growth models.

Reproduction

Kawaguchi *et al.* (2007b) developed a conceptual model of the synchronization of reproduction and growth in krill to the seasonal cycle of light, food, sea ice, and temperature. This cycle primarily relates to female krill in terms of gonadal investment because male gonad size makes little difference to the overall dry mass of male krill (Morris *et al.*, 1988). For our EMC model below, we formalized this conceptual model into a sequence of three phases in the annual reproductive cycle of female adult krill.

The *post-regression phase* is a fixed period after regression of approximately five moult cycles to enable the body to mature in readiness for gonadal development.

The *reproductive phase* is when gonads increase in size and eggs mature over at least two moults, giving rise to spawning after two moults if a critical gonad mass is achieved. If the critical gonad mass is not achieved then the investment may continue to be accumulated in subsequent IMPs to be spawned at a later moult once the critical mass is achieved. Multiple spawnings may occur in one season if sufficient energy is invested in the gonads after a spawning.

The *regression phase* begins as a result of either insufficient resources invested in the gonad later in the season (more than two moults since the last spawning) or insufficient day length causes rapid regression to occur (Brown *et al.*, 2010). The regression period is expected to end no later than three moult cycles after the critical day length occurs in the austral autumn but will be no longer than five moult cycles after it begins (Brown *et al.*, 2011).

Energetics

Energetic models differentiate the amount of food consumed into metabolism, growth and reproduction (e.g. Hofman and Lascara, 2000; Alonzo and Mangel, 2001). Laboratory experiments are used to derive the necessary energetic and physiological parameters. These models often convert mass to length or length to mass.

The model of Hofman and Lascara (2000) is a time-dependent, size-structured, physiological krill growth model used to explore the consistency of experimental and laboratory measurements of krill metabolic processes and to evaluate the processes by which krill over-winter. Fach *et al.* (2006) used a modified version coupled to a circulation model for the Scotia Sea to test whether krill could be sustained while being transported from the Antarctic Peninsula to South Georgia. Although these models provide flexibility in understanding growth trajectories, they have, to date, not accounted for moult cycles and the phases in the annual reproductive cycle.

Dynamic energy budget theory (DEB) has been used to model Antarctic krill growth to investigate how spatio-temporal sea ice dynamics, food availability and chronobiology may affect krill distribution and its population dynamics (Groeneveld *et al.*, 2015; Jager and Ravagnan, 2015). DEB relies on a set of parameters to characterize the specifics of metabolic organization and physiology, and life history, based on thermodynamic principles. These parameters cannot be measured directly but are estimated from experimental data. As with other energetic models, its current formulation tightly couples length and mass of krill. The approach also does not include other important aspects of species biology and ecology (Galic and Forbes 2017), which could be limiting for general applications given the synchronicity of krill to the annual cycle.

In a similar way, a bioenergetics life history model for krill has been developed to explore the effects of environmental factors on the population dynamics of krill (Ryabov *et al.* 2017). In this case, a primary source of variation in the krill population was due to intraspecific competition for food. Their krill model assumes growth, maturity, and fecundity of krill depend on the food level and their size and stage. The model was formulated to partition resources between growth and reproduction using a size-dependent logistic function, which is set to divert 100% of the resources to reproduction at 70 mm and thereby not allowing krill to grow beyond that size. The body length and mass were also tightly coupled; the model is not able to represent thinning or fattening of the body which are indicative of the health of the animal.

A moult cycle model based on energetics

The coupled EMC model for krill combines an energetics model for the IMP with the requirements of the moult cycle, the constraints of the annual cycle, and the role that the size of the exoskeleton plays in determining feeding rates, limiting growth in length (both positive and negative) and fecundity.

Energetics during the IMP

Typically, the energetics model is based on units of mass and partitions ingested food into metabolism and reserves for body growth and reproduction [Table 2, Equation (2.1)]. During the IMP, the size of the exoskeleton is fixed from the previous moult, thereby setting the feeding rate and the constraints on growth and

Table 2. Equations and parameters for energetics over an IMP used in the EMC model of productivity in Antarctic krill.

Name	No.	Equation	Parameters
Basic energetics model	2.1	$A = M + dB + G$	A, assimilated energy; M, metabolism and maintenance; dB, investment in body mass; G, investment in gonads
Assimilated energy (A)	2.2	$A = f(L, I, \epsilon)$	Function. L, body length (mm); I, amount ingested; ϵ , assimilation efficiency, given amount ingested.
Food Ingestion (I)	2.3	$I = f(L, FA, B)$	Function. FA, food available; B, Body mass at start of IMP
Metabolism (M)	2.4	$M = f(B, T, \alpha)$	Function. T, Temperature ($^{\circ}\text{C}$); α , activity.
Body outputs	2.5	$F = I - A$	F, egestion (faeces); N, excretion (nitrogenous waste).
Total reserves (A')	2.6	$N = f(M)$ $A' = (B + G - \bar{B} - m) + (A - M)$	G, Gonad mass at IMP start; \bar{B} , Healthy body mass able to grow and reproduce; m, cost of discarded moult at end of IMP.
Maxima of reserves for positive growth ($d\hat{B}_p$) and reproduction (\hat{G})	2.7	$d\hat{B}_p = f(L, \bar{B})$ $\hat{G} = f(L)$	
Total reserves adjusted (A'')	2.8	$A'' = A'$ if $[A' \leq (d\hat{B}_p + \hat{G})]$ $A'' = (d\hat{B}_p + \hat{G})$ if $[A' > (d\hat{B}_p + \hat{G})]$	
Proportion reserves allocated to reproduction (P)	2.9, 16	$P = f(\text{sex, maturity, } L, \bar{B}, \text{Gphase})$	Gphase, phase in the gonadal cycle.
Reserves for growth (dB)	2.10	$dB = A''(1 - P) + G'$ if $[(A''(1 - P) + G') \leq d\hat{B}_p]$ $dB = d\hat{B}_p$ if $[(A''(1 - P) + G') > d\hat{B}_p]$	
Reproduction reserves (G)	2.11	$G = A''P + dB'$ if $[(A''P + dB') \leq \hat{G}]$ $G = \hat{G}$ if $[(A''P + dB') > \hat{G}]$	
Excess growth reserves (dB')	2.12	$dB' = A''(1 - P) - d\hat{B}_p$ if $[A''(1 - P) < d\hat{B}_p]$ $dB' = 0$ otherwise	The algorithm does not allow dB' to be greater than $[\hat{G} - A''P]$.
Excess reproduction reserves (G')	2.13	$G' = A''P - \hat{G}$ if $[A''P < \hat{G}]$ $G' = 0$ otherwise	Algorithm does not allow G' to be greater than $[d\hat{B}_p - A''(1 - P)]$.

Units are mgC unless otherwise indicated. The equations relate to the algorithm illustrated in Figure 2.

reproduction. The energetics algorithm is illustrated in Figure 2 and the equations and definitions are elaborated in Table 2.

Assimilated mass is governed by the ingestion of food, which is primarily a product of filtration rate and food concentration, and the assimilation efficiency. The latter may also be affected by the rate of ingestion; greater ingestion rates may result in decreased efficiency. Egestion (faeces) is the food value left over after assimilation. In the absence of appropriately calibrated assimilation efficiencies, the model has a post-hoc adjustment of egestion which is the assimilated mass in excess of that required for metabolism and the maxima in positive growth and gonad size (Figure 2).

Metabolism is an energetic cost of activity and maintenance of the animal. It is determined by the mass of the krill and the level of activity and movement. Metabolism is positively correlated with temperature of the water. Excretion of nitrogenous waste is a product of metabolism.

We use the gonads as a dynamic energy reserve when the gonadal phase permits investment in the gonad. The body also has a dynamic reserve but its weight, relative to length, will determine the health of the animal, which is a threshold requirement for positive growth and reproduction. The total reserves available at the end of an IMP will be determined by the combined initial body and gonad mass less the minimum mass needed to have a healthy body, less the cost of the discarded moult, in addition to the

assimilated energy less the amount expended in metabolism. If the total reserves are calculated to be less than zero then the krill is starving, cannot reproduce, and the exoskeleton will shrink at the moult.

If the body mass has met the threshold for health, three factors will govern the total investment in each of positive growth and reproduction—the maximum possible growth in the exoskeleton, the maximum possible size of the gonads and the proportional allocation of the excess reserves between growth and reproduction. The roles of each of these quantities are shown in Figure 2 and Table 2. They are further described in the Methods section.

Moult cycle governing growth and reproduction

The moult cycle results in punctuated growth governed by the length of the IMP. The IMP model [Table 1, Equation (1.5)] of Kawaguchi *et al.* (2006) is used in the EMC model. At the time of moulting, the body reserve is converted to a change in length [Table 3, Equation (3.1)]. Here, the body reserve is relative to the body mass considered to be the minimum required for the pre-moult krill to be healthy. If the body reserve is less than the healthy mass, i.e. thin krill, then the animal will shrink. If it is greater than the healthy mass, i.e. fat krill, then the animal will have positive growth. As per the limits on positive growth above,

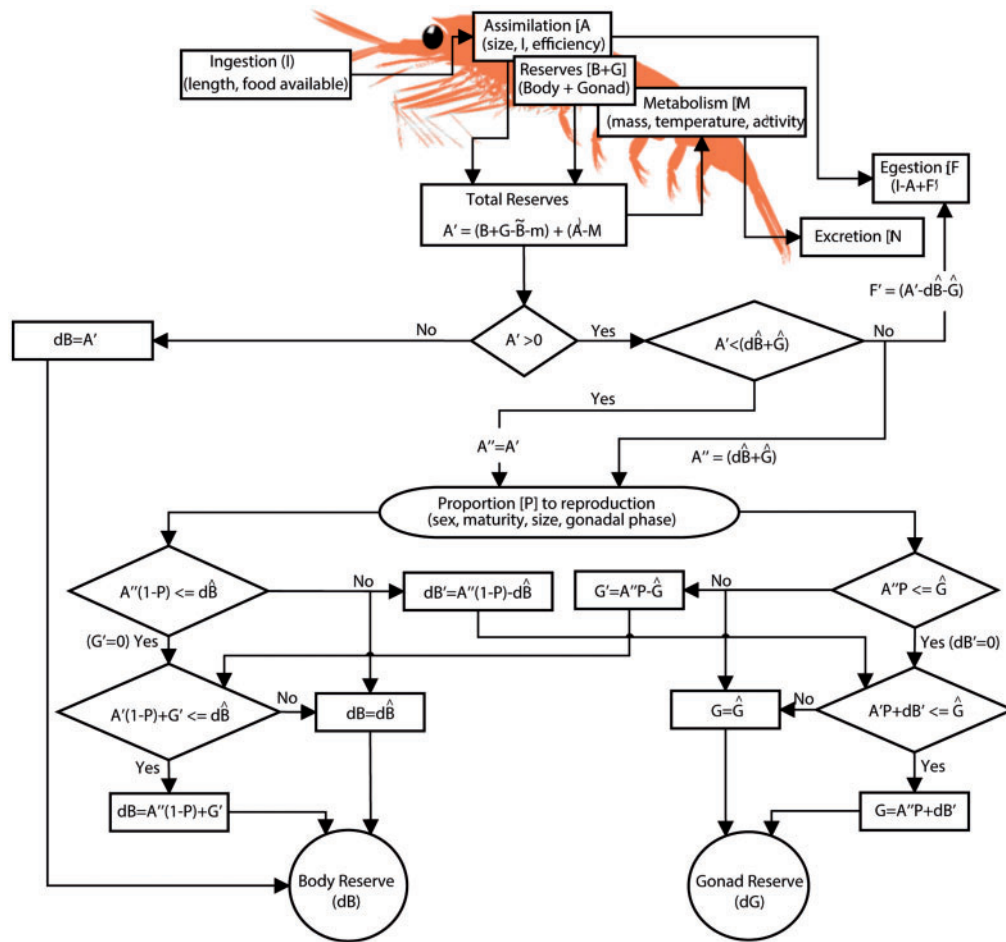


Figure 2. Flow chart showing the partitioning of ingested food between metabolism, growth and reproduction during the IMP in the EMC model for Antarctic krill. Symbols are defined in Tables 2 and 3.

the maximum body reserve can be no more than what is needed to achieve the maximum possible growth increment for that pre-moult length.

Starving krill can shrink the exoskeleton but only up to a maximum proportion of length per day. If maximum shrinkage has occurred and the new body mass is less than for a healthy krill then thin krill will be the outcome. In this model, thin krill must recover to a healthy mass before positive growth and/or reproduction can occur. Body mass relative to the size of the exoskeleton may continue to decline under low food scenarios and result in mortality from starvation.

If the gonad is in the reproductive phase and the moult is after two IMPs then it will be converted to reproductive output as eggs and the gonad reserve is reset to zero [Table 3, Equation (3.2)]. If only after one IMP then the gonad remains as a reserve. If the reserve has not been expended when the reproductive cycle moves to the regression phase then the remaining gonad reserve can be used, if needed, to supplement metabolism and growth.

Methods

Derivation of parameters

The model developed here uses carbon (mgC) as the unit of mass for the energetics model, as this is the measure most readily

available for all components of the model. We use morphometric equations to derive dry mass at length and maximum dry mass of a gonad at length for a healthy krill [Table 4, Equations (4.1) and (4.2)] and convert these to carbon mass [Table 4, Equations (4.3) and (4.4)].

Ingested carbon for a given length of krill [Table 2, Equation (2.3)] is determined from the filtration rate, the available concentration of carbon in the water being filtered, and the length of time filtering the water [Table 4, Equations (4.5 and 4.6)]. We use the filtration rate model of Hofmann and Lascara (2000), which relates filtration rate to dry body weight. Here, we determine the dry weight from length using Equation (4.1), assuming thin krill and healthy krill have approximately the same filtration rates. We acknowledge that the filtration rate may decline with very high densities of food (Quetin and Ross, 1985) but do not include that here or any selectivity for a range of particle types.

The proportion of ingested resources assimilated (assimilation efficiency) is fixed at 0.8 [Table 4, Equation (4.7)]. We have not modelled the potential decline in assimilation efficiency with increasing ingestion, which may occur because of an increased rate of passage of material through the gut.

Metabolism per day [Table 2, Equation (2.4)] is determined by, first, calculating respiration using the function of Ikeda

Table 3. Equations and parameters for growth, reproduction, and designation of phases in the annual cycle that occur at the time of moulting in the EMC model for Antarctic krill.

Name	No.	Equation or component	Parameters
Change in length and mass	3.1	$L_{i+1} = \begin{cases} L(\bar{B} + dB) & d\hat{B}_s \leq dB \leq d\hat{B}_p \\ L_i - d\hat{L}_s & dB < d\hat{B}_s \end{cases}$ $B_{i+1} = \bar{B} + dB$	$L(\bar{B} + dB)$ is length for a healthy krill given a mass $d\hat{L}_s$ and $d\hat{B}_s$ are the maximum shrinkage that can occur and the corresponding change in mass to retain health respectively.
Reproductive output	3.2	$R = \left(\frac{G}{G}\right)\hat{R}$	
Gonadal Phase (<i>Gphase</i>)		Males	$P = 0$
		Immature females	$P = 0$
		Mature females	
		Ovarian cycle	Onset: $P = 0.8$
		Regression	Onset: $P = 0$
		Post-regression	Onset: $P = 0$

(1974), which accounts for the relationship with temperature, and then using the conversion to *mgC* of Hofmann and Lascara (2000) [Table 4, Equation (4.8)]. Here the actual weight of the krill is used rather than inferring dry weight from its length, i.e. thin krill will have a lower metabolic requirement than healthy krill. The results of Ikeda and Thomas (1987) for growth in juvenile krill were examined to see if they could be used to estimate the conversion ratio. However, the results presented in their paper were insufficient to derive the necessary data for these calculations.

The maximum growth increment at length [Table 4, Equation (4.10)] used in the implementation of our model was determined from two least-square regressions—positive growth and negative growth. The positive growth regression was estimated from IGRs for krill juveniles, males and females measured in the Indian Sector of the Southern Ocean in December (Kawaguchi *et al.*, 2006). For animals that shrink, a regression of the maximum daily shrinkage in length against length was estimated from the limited data available in Figure 1 from Ikeda and Dixon (1982), which were from an experiment where animals were not fed over the life of the experiment. The new lengths are converted to a maximum change in mass using the morphometric equation for healthy krill.

At the time of the moult, the new length is determined as the length that corresponds to the post-moult healthy carbon mass of the krill [Table 3, Equation (3.1)]. For shrinking animals, the new length cannot be less than the maximum shrinkage possible, even though the body mass may then be less than the healthy mass. The cost of replacing the exoskeleton after a moult [Table 2, Equation (2.6)] was determined as the expected carbon content of the lost exoskeleton, which is determined as the proportion of body dry weight of a healthy animal that is the exoskeleton (Nicol *et al.*, 1995) and then converting this to carbon (Ikeda, 1984) [Table 4, Equation (4.9)].

Thin krill may eventually die from starvation if their body condition relative to the length of krill declines below a threshold level. At present, krill die when the body mass reduces to zero.

The transitions between the three different phases of the reproductive cycle described earlier were implemented as follows. During the reproductive phase, spawning occurs every second moult if the gonad reserves are greater than the critical mass of 10% of the maximum possible (Nicol *et al.*, 1995). If the critical gonad mass is not achieved then the gonad reserves are carried

over into the next IMP. The regression phase begins if (i) there have been more than four moults since the last spawning, (ii) there has been two moults since the last spawning and the day length is shorter than 5 h, or (iii) the day length has become shorter than the critical day length of 2 hours. In the last case, the regression period will end three moult cycles after the critical day length occurs in the austral autumn. In the first two cases, it will end after five moult cycles (Brown *et al.*, 2011). The post-regression phase is a fixed period after regression of five moult cycles, after which the reproductive phase occurs.

For implementing reproduction, we assume the proportion to reproduction is zero in both juveniles and males at all times and in females during the regression period over winter (Kawaguchi *et al.*, 2007b) [Table 2, Equation (2.9)]. For females in the reproductive period, the proportion allocated to reproduction, if unknown, can be used as a tuning parameter. We do not know what this proportion should be and set the allocation to reproduction to 0.95.

Maximum investment in the gonad for a given length [Table 2, Equation (2.7)] is determined by combining Equations (4.2) and (4.4) based on the morphometrics of Morris *et al.* (1988). For spawning, gonads greater than the critical mass [Table 3, Equation (3.2)] are converted to eggs by transforming the gonad to energy and dividing by the energy contained within an egg (Nicol *et al.*, 1995) [Table 4, Equation (4.11)]. We use this approach in order to take account of investment in gonad mass, compared with other approaches which have developed regressions of eggs against female body length. We have not yet factored in the energetic cost of producing eggs due to the absence of such estimates. This will be useful in the future to improve the accuracy of the model.

Evaluating the EMC model

The EMC model was implemented using the statistical programming language, R Development Core Team (2017). Two experiments were undertaken to evaluate whether the model performed according to expectations.

Modelling experiment 1

The performance of the EMC model was evaluated, first, using temperature and food conditions from the west of South Georgia, where much of the expectations for growth in krill have been

Table 4. Derivation of parameter values and functions used to implement the EMC model for Antarctic krill.

Name	No.	Equation or component	Parameters	Source
Dry mass (g) at length (mm)	4.1	$W_s(L) = d_{1,s}(a_s L^{b_s}) + d_{2,s}$	Stage (s) a_s b_s $d_{1,s}$ $d_{2,s}$ Male (M) 21.38 E-6 2.76 0.195 -0.014 Female (S1) 30.20 E-6 2.62 0.251 -0.013 Female (S4) 9.77 E-6 2.98 0.275 -0.014	Morris <i>et al.</i> (1988)
Gonad dry mass (γ , g) at length (mm)	4.2	$\hat{R} = \gamma(L) = W_{S4}(L) - W_{S1}(L)$		
Conversion of body dry mass to carbon mass	4.3	$C(W) = \alpha W^\beta$	$\alpha = 0.366; \beta = 1.037$	Hofmann and Lascara (2000)
Conversion of gonad dry mass to carbon mass	4.4	$C(\gamma) = \alpha \gamma$	$\alpha = 0.551$	Ikeda (1984)
Filtration (m^3) rate per day given length (mm)	4.5	$R_s(L) = \begin{cases} \alpha_1 W_s(L)^{\beta_1} & W_s(L) < w_1 \\ d_1 \alpha_1 W_s(L)^{\beta_1} + d_2 \alpha_2 W_s(L)^{\beta_2} & w_1 \leq W_s(L) \leq w_2 \\ \alpha_2 W_s(L)^{\beta_2} & W_s(L) < w_2 \end{cases}$ <p>where</p> $d_1 = \frac{(w_2 - W_s(L))}{w_2}; \quad d_2 = \frac{(W_s(L) - w_1)}{w_1}$	$w_1 = 26 \text{ mg}; \alpha_1 = 8.5\text{E-}5; \beta_1 = 0.825$ $w_2 = 84 \text{ mg}; \alpha_2 = 3.43\text{E-}4; \beta_2 = 0.514$	Hofmann and Lascara (2000)
Ingestion (mgC) per day at length (mm)	4.6	$I_s(L) = R_s(L)C_w$	$C_w = \text{carbon concentration (mgC.m}^{-3}\text{)}$	
Assimilated carbon (mg) per day at length (mm)	4.7	$A_s(L) = \alpha I_s(L)$	$\alpha = 0.8$	Hofmann and Lascara (2000)
Metabolism (mgC) per day	4.8	$M(B) = 24\beta(10^{c_1 T + c_2} B^{c_3 T + c_4})$	$B = \text{actual body mass}; \beta = 1/535.7 \text{ ul O}_2.\text{mgC}^{-1}; c_1 = 0.02438; c_2 = -0.1838; c_3 = -0.0109; c_4 = 0.8918$	Ikeda (1974), Hofmann and Lascara (2000)
Carbon mass (mgC) of an exoskeleton (mm)	4.9	$m_s(L) = p_c p_w W_s(L)$	$p_w = 0.075; p_c = 0.238$	Ikeda (1984), Nicol <i>et al.</i> (1995)
Maximum growth—Length $d\hat{L}_g$, Mass ($d\hat{B}_g$)	4.10	$d\hat{L}_g(L) = \alpha_g - \beta_g L$ $d\hat{B}_g = W(L_i + d\hat{L}_g(L_i)) - W(L_i)$	$g = p \text{ (positive) or } s \text{ (shrink)}$ $\alpha_p = 8.63; \beta_p = 0.14; \alpha_s = 1.3\text{E-}3; \beta_s = 1.418\text{E-}5$	Positive—Kawaguchi <i>et al.</i> (2006) Shrink—Ikeda and Dixon (1982)
Eggs from gonad mass (mg)	4.11	$\text{Eggs} = \frac{Jg^R}{J_e}$	$R = \text{gonad mass (mg) from Table 3, Equation 22}$ $Jg = \text{energy content (J.mg}^{-1}\text{) of ovarian tissue} = 25.8$ $J_e = \text{energy content (J) of an egg} = 0.6824$	Nicol <i>et al.</i> (1995)

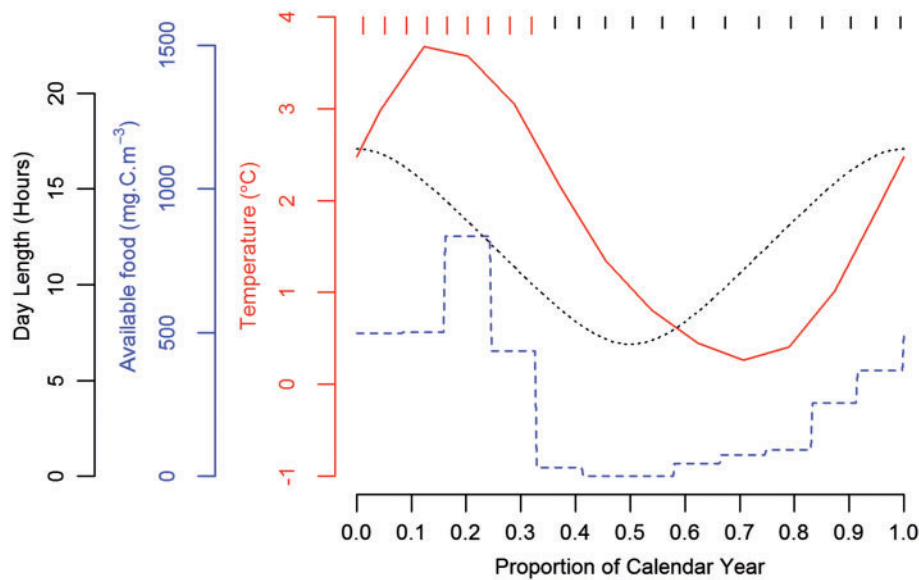


Figure 3. Average annual cycles over a calendar year for mean monthly sea surface temperature ($^{\circ}\text{C}$) (solid line), mean monthly Chlorophyll *a* concentration (mg.m^{-3}) as available food (dashed line) and day length (hours of sunlight) (dotted line) for the West South Georgia Small Scale Management Unit of CCAMLR. Vertical lines at the top show the timing of moults through the year according to the IMP model of Kawaguchi *et al.* (2006). Longer lines show the IMPs when gonad size is greater than zero for Age 5 krill in the projections shown in Figures 4 and 5.

derived. We use satellite data for the area bounded by the west South Georgia small-scale management unit of CCAMLR (SC-CAMLR, 2002).

SeaWiFS ocean colour data (SeaWiFS Chlorophyll *a*, SeaWiFS, 2005) for the period September 1997 to December 2004 were used to derive monthly means of sea surface Chlorophyll *a* density as a proxy for the density of phytoplankton available for consumption. Sea surface temperature (NOAA OIv2 SST, Reynolds *et al.*, 2002) for the period December 1981 to May 2006 were used to derive monthly means of temperature. These two parameters along with the cycle of day length for the area provide average annual cycles of sea-surface temperature ($^{\circ}\text{C}$), carbon density derived from Chlorophyll *a* density (mg.m^{-3}), and day length, which are all important in the application of the EMC model (Figure 3).

Using the annual cycles of temperature, food and day length, the EMC growth model was projected from ages 1 to 9 years with a starting length at Age 1 of 20 mm and a corresponding healthy dry weight for males and females, respectively.

Modelling experiment 2

A second modelling experiment was undertaken to examine how krill growth and reproduction varied using the EMC model under specific temperature and food conditions. Four lengths of krill (30, 40, 50, 60 mm) were projected for 1 year under constant conditions. Temperature conditions were in 0.1°C intervals from -1 to 5°C . Food conditions were at 0.05 (low food), 0.5 (medium food), and 1.0 (high food) times a food density (mgC.m^{-3}) that was just limiting for the 30 mm length class. Projections were undertaken separately for males and females.

Results

Modelling experiment 1

The results (length at age) for a male growth model (no reproduction) and a female growth model (reproduction for ages >2) are shown in Figure 4, along with the average length at age. This

result is achieved by scaling the feeding efficiency to 0.063 of the food in the cycle in Figure 3 and for the allocation of resources to reproduction to be set at 0.95. Dry weights (mg) for males and females are also shown, along with the number of eggs produced in each batch spawned over the life of the krill.

The mean length at age shows the typical expectation for krill at South Georgia, with a punctuated growth form similar to that of Rosenberg *et al.* (1986) and Candy and Kawaguchi (2006). It also shows that shrinkage can occur in the exoskeleton but not as much as may be expected by the fluctuation in body mass, which mirror the food cycle for the area. These fluctuations show the potential for observing thin krill during the austral winter and early spring.

The number of batches and number of eggs per batch for the different age classes are also indicative for krill in this area; younger females may produce up to five batches in a season with approximately two thousand eggs in some batches, which is consistent with field observations in the region (Tarling *et al.*, 2007).

Figure 5 presents the trajectories for length, body dry weight, and gonad dry weight for Age 5 krill over one year. This figure shows the overall behaviour of the model with respect to changes in the exoskeleton and energetics in relation to the moult and reproductive cycles impacted by the variations in food, temperature and light.

Modelling experiment 2

The results for the second modelling experiment are illustrated as the proportional change in length over one year in Figure 6 and the total number of eggs produced by females over the year in Figure 7.

Close inspection of the low (0.05) food scenario in Figure 6 shows that all krill shrank at this food level. Although not illustrated here, the ratio of dry weight after 1 year to the dry weight at the beginning for all krill steadily declined with increasing temperature. The temperature at which the body condition at the end of the year became zero is when the proportional change in length became zero. This

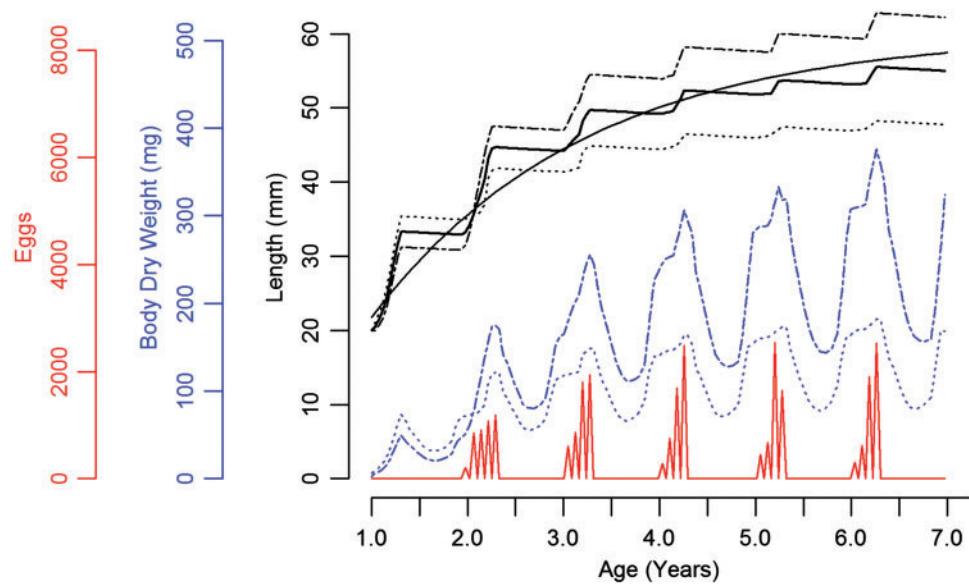


Figure 4. Results of the first simulation experiment projecting 1-year old Antarctic krill for 6 years using the EMC model, based on the annual cycle of temperature, food and day length given in Figure 3, with the efficiency of food acquisition the same for all ages. The trajectories of three attributes of the krill relative to age are shown: lengths (mm) (four lines at top); body dry weight (mg) (two lines at centre), and eggs (line at bottom). Results are separated for males (dot-dash line) and females (dotted line) for length and dry weight. At top, the average length combining males and females is shown with a thick solid line to compare with the vB model from Figure 1 (thin solid line).

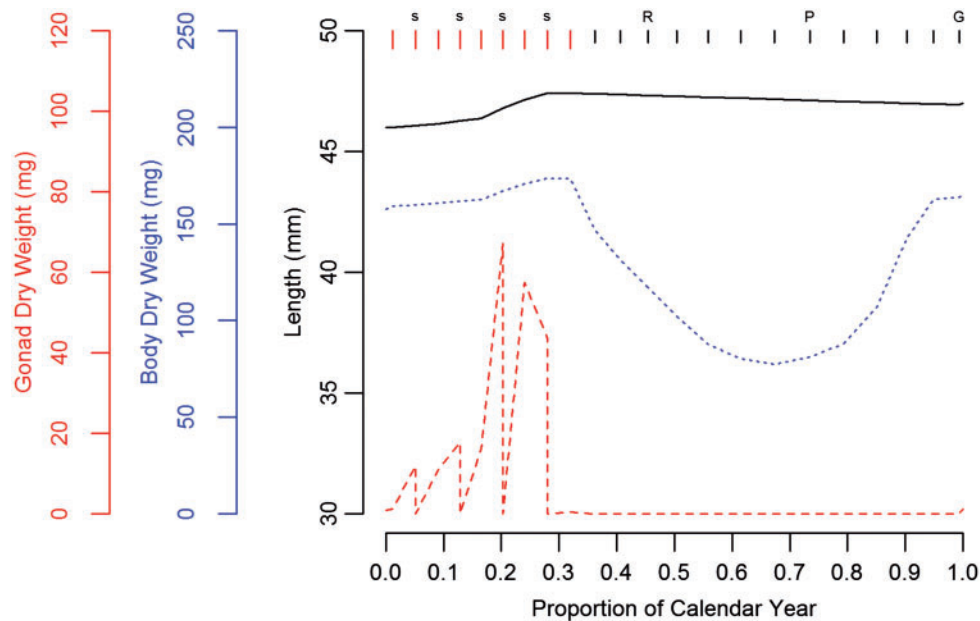


Figure 5. An 1-year projection of attributes of female Age 5 Antarctic krill from Figure 4. Length (mm) (solid) and body dry weight (mg) (dotted) are the same. Gonad dry weight (mg) (dashed) is shown in place of the eggs. Vertical lines at the top are the same as in Figure 3, showing the timing of the moults. Letters above those lines represent the start of the different phases of the reproductive cycle—G is for the gonadal development during the reproductive phase, R is the start of regression, P is the start of the post-regression phase, and s indicates spawning at moult.

decrease in body condition with temperature was faster in larger krill than with smaller krill, indicating that larger krill were more vulnerable to starvation with increasing temperatures than smaller krill, because of their greater relative metabolic demand.

For the two greater food levels, the proportional changes in length differ between males and females because of the investment in reproduction by females. At the 0.5 food level, the 50 and

60 mm krill were unable to grow or reproduce while the smaller reproductive krill performed much better, maintaining some positive annual growth even at higher temperatures. Annual egg production tended to decline in 40 mm krill compared with 30 mm krill, also as a result of increased metabolic cost. The results for the 0.5 food level show that reproductive output is maintained at the expense of growth.

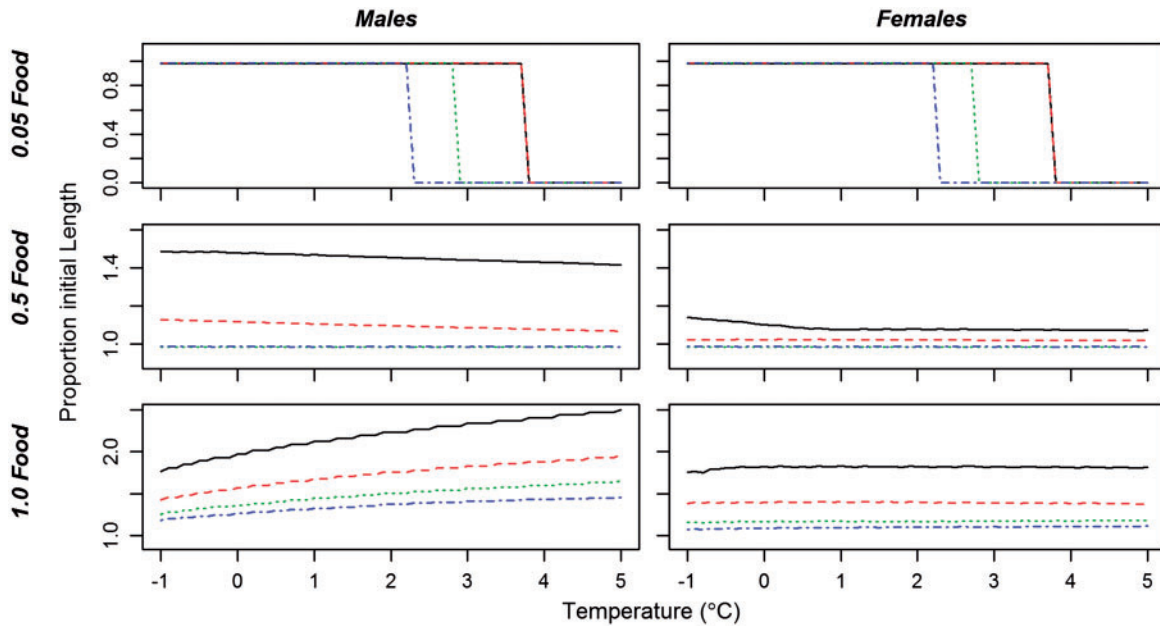


Figure 6. Proportional changes in length of Antarctic krill in the second simulation experiment. Four different lengths of mature female and male krill were projected for one year in different combinations of constant food and temperature. Initial lengths were 30 mm (solid line), 40 mm (dashed), 50 mm (dotted) and 60 mm (dot-dash). Proportional changes are the lengths at the end of one year as a proportion of the starting length. Proportional changes are plotted against temperature ($^{\circ}\text{C}$). Columns of panels show results for males (left) and females (right) with three rows of relative food availability: top—very low (0.05 of maximum), mid—medium (0.5), and bottom—high (1.0).

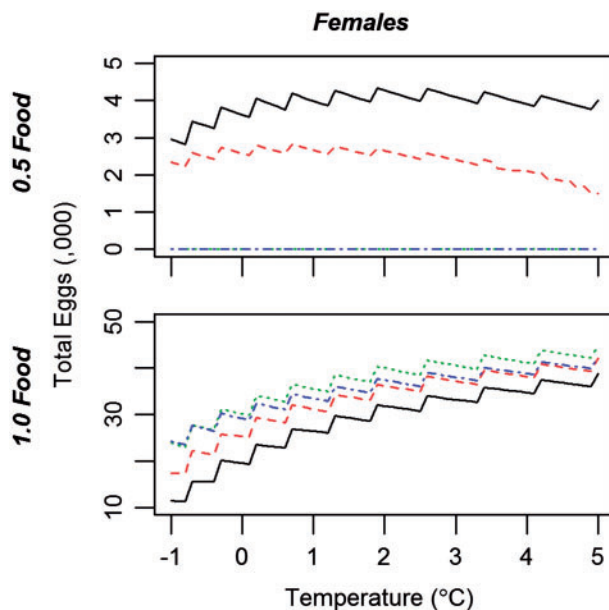


Figure 7. Total eggs produced by mature females over one year in the second simulation experiment. Explanation of the experiment are in Figure 6. Total eggs plotted against temperature ($^{\circ}\text{C}$). Results only shown for females with two levels of food availability: top—medium (0.5) and bottom—high (1.0). No eggs were produced in the treatments with low (0.05) food availability.

In high food (just limiting for 30 mm krill) conditions, the increasing growth with temperature of the four lengths of males is a result of the shortening of the IMP at higher temperatures. The stepwise nature of this relationship occurs because of the addition

of a moult into the annual cycle, resulting in a greater size, greater food acquisition, and larger egg production. Although this is true for the females at lower temperatures, the lower growth at higher temperatures and the declining egg production after the addition of each moult to the annual cycle demonstrates the effects of increasing metabolism with temperature. In this experiment, growth for females is greatest in the temperature range of -0.5 and 1°C , suggesting this temperature range may be the ideal habitat for Antarctic krill, consistent with field observation by Atkinson *et al.* (2006). Egg production follows expected trends associated with temperature and food, with recent estimates of $\sim 12,000$ eggs per year per individual at South Georgia, where food would be expected to be limiting (compared with the food level here) and would only be available for a summer growth period (Tarling *et al.*, 2007).

Discussion

Models of krill growth are expected to show an annual cycle of rapid growth in spring and summer and little growth in winter with the overall annual increment reducing as reproduction becomes a priority. The expectation is that krill will have a maximum size between 50 and 60 mm in length. Our EMC model performs well against these expectations. It provides the flexibility for use outside of the domain in which the IGR data were obtained by being able to utilize food and temperature data in the model and successfully return plausible life history responses (e.g. growth, fecundity). It also means that growth and reproduction can more realistically respond to changes in the density of the population as well as changes in the environment. This flexibility in growth is supported by recent estimates of the variability in length at age from eye-stalk annual growth bands, which indicate that krill, in the field, are very plastic in their growth (Kilada *et al.*, 2017).

The difference between male and female length at age in the EMC model reflect observations and expectations from life history theory. The male growth trajectory is very similar to that recorded from field observations by Kawaguchi *et al.* (2007a). Also, investment in male gonads is only small, which would result in more energy for growth. The asymptote for males is governed by the metabolic requirements for large bodies. For females, the diversion of energy to reproduction will slow the growth rate. In large females, the size of the gonad is also very large, requiring a large diversion of resources from growth. Thus, mature females are expected to be smaller in length at age than males.

vB-class growth models are comparatively inflexible and are not likely to be suitable for population assessments on the scale of whole krill populations due to large regional variability in temperature and food. Continued use of these types of models would require a re-estimation of the parameters for different regions and periods.

Empirical models of growth rate based on IGR methods are better than the vB class at larger spatial and temporal scales. Current models will require further empirical evidence and more detail in the models to address the probable interactions between temperature, food, environmental conditions, density of krill and maturity stage.

The EMC model presented here utilizes field observations of growth and takes account of important factors varying in space and time, notably temperature and food. The potential for ingestion rates to differ between areas or times because of changes in phytoplankton size and/or availability will be important to consider for the model to appropriately represent the responses of krill under the respective circumstances. Intra-specific competition will also be an important factor to consider in calculating ingestion rates. Other useful additions to this model in future will be to account for the energetic cost of movement of krill, how ingestion and assimilation may be impacted by different densities of food, and the energetic cost of producing body mass and eggs.

Overall, the parameterization for the EMC model provides results consistent with expectations, with flexibility for application to spatially and temporally varying conditions as will be experienced in the future. We recommend that this new model be incorporated into assessments of precautionary yield for Antarctic krill.

Acknowledgements

This article evolved from work presented to CCAMLR WG-EMM in 2005–2006. We thank many participants of WG-EMM for their feedback. We particularly thank Steve Candy and Steve Nicol for discussions over a number of years on the drivers of growth in krill. Thank you to Mike Sumner for assistance with the satellite data. Thanks to Dirk Welsford, Jess Melbourne-Thomas, Rowan Trebilco, Stéphane Plourde, and two anonymous reviewers for comments on the article. Sea-surface temperature data were made available by US NOAA. Chlorophyll *a* data were made available by the SeaWiFS Project (Code 970.2) and the Distributed Active Archive Center (Code 902) at the Goddard Space Flight Center, Greenbelt, MD 20771. The algorithm for the EMC function is available in R-script. A.C. was supported in part by a Pew Fellowship in Marine Conservation.

References

Alonzo, S. H., and Mangel, M. 2001. Survival strategies and growth of krill: avoiding predators in space and time. *Marine Ecology Progress Series*, 209: 203–217.

- Aseev, Y. 1984. Size structure of krill populations and life span in the Indian Ocean sector of the Antarctic. *Hydrobiological Journal*, 20: 89–94.
- Atkinson, A., Shreeve, R. S., Hirst, A. G., Rothery, P., Tarling, G. A., Pond, D. W., Korb, R. E. *et al.* 2006. Natural growth rates in Antarctic krill (*Euphausia superba*): II. Predictive models based on food, temperature, body length, sex, and maturity stage. *Limnology and Oceanography*, 51: 973–987.
- Atkinson, A., Siegel, V., Pakhomov, E. A., Rothery, P., Loeb, V., Ross, R. M., Quetin, L. B. *et al.* 2008. Oceanic circumpolar habitats of Antarctic krill. *Marine Ecology Progress Series*, 362: 1–23.
- Brown, M., Kawaguchi, S., Candy, S., and Virtue, P. 2010. Temperature effects on the growth and maturation of Antarctic krill (*Euphausia superba*). *DSRII Krill biology and ecology. Deep-Sea Research II*, 57: 672–682.
- Brown, M., Kawaguchi, S., King, R., Virtue, V., and Nicol, S. 2011. Flexible adaptation of the seasonal krill maturity cycle in the laboratory. *Journal of Plankton Research*, 33: 821–826.
- Candy, S. G., and Kawaguchi, S. 2006. Modelling growth of Antarctic krill: II. Novel approach to describing the growth trajectory. *Marine Ecology Progress Series*, 306: 17–30.
- Constable, A. J. 2011. Lessons from CCAMLR on the implementation of the ecosystem approach to managing fisheries. *Fish and Fisheries*, 12: 138–151.
- Constable, A. J., and de la Mare, W. K. 1996. A generalised model for evaluating yield and the long term status of fish stocks under conditions of uncertainty. *CCAMLR Science*, 3: 31–54.
- Constable, A. J., de la Mare, W. K., Agnew, D. J., Everson, I., and Miller, D. 2000. Managing fisheries to conserve the Antarctic marine ecosystem: practical implementation of the Convention on the Conservation of Antarctic Marine Living Resources (CCAMLR). *ICES Journal of Marine Science*, 57: 778–791.
- Constable, A. J., Melbourne-Thomas, J., Corney, S. P., Arrigo, K. R., Barbraud, C., Barnes, D. K. A., Bindoff, N. L. *et al.* 2014. Climate change and Southern Ocean ecosystems I: how changes in physical habitats directly affect marine biota. *Global Change Biology*, 20: 3004–3025.
- Fach, B. A., Hofmann, E. E., and Murphy, E. J. 2006. Transport of Antarctic krill (*Euphausia superba*) across the Scotia Sea. Part II: Krill growth and survival. *Deep Sea Research Part I: Oceanographic Research Papers*, 53: 1011–1043.
- Galic, N., and Forbes, V. E. 2017. The role of Dynamic Energy Budget theory in predictive modelling of stressor impacts on ecological systems: Comment on: “Physics of metabolic organisation” by Marke Jusup. *Physics of Life Reviews*, 20: 43–45.
- Groeneveld, J., Johst, K., Kawaguchi, S., Meyer, B., Teschke, M., and Grimm, V. 2015. How biological clocks and changing environmental conditions determine local population growth and species distribution in Antarctic krill (*Euphausia superba*): a conceptual model. *Ecological Modelling*, 303: 78–86.
- Hartnoll, R. G. 2001. Growth in crustacean—twenty years on. *Hydrobiologia*, 449: 111–122.
- Hill, S. L., Phillips, T., Atkinson, A., and Browman, H. I. 2013. Potential climate change effects on the habitat of Antarctic krill in the Weddell quadrant of the Southern Ocean. *PLoS One*, 8.8: e72246.
- Hofmann, E. E., and Lascara, C. M. 2000. Modeling the growth dynamics of Antarctic krill *Euphausia superba*. *Marine Ecology Progress Series*, 194: 219–231.
- Ikeda, T. 1974. Nutritional ecology of marine zooplankton. *Memoirs of The Faculty of Fisheries, Hokkaido University*, 22: 1–97.
- Ikeda, T. 1984. Sequences in metabolic rates and elemental composition (C, N, P) during the development of *Euphausia superba* Dana and estimated food requirements during its life span. *Journal of Crustacean Biology*, 4: 273–284.
- Ikeda, T., and Dixon, P. 1982. Body shrinkage as a possible over-wintering mechanism of the Antarctic krill, *Euphausia*

- superba* Dana. Journal of Experimental Marine Biology and Ecology, 62: 143–151.
- Ikeda, T., Dixon, P., and Kirkwood, J. 1985. Laboratory observations of moulting, growth and maturation in Antarctic krill (*Euphausia superba* Dana). Polar Biology, 4: 1–18.
- Ikeda, T., and Thomas, P. G. 1987. Moulting interval and growth of juvenile Antarctic krill (*Euphausia superba*) fed different concentrations of the diatom *Phaeodactylum tricornutum* in the laboratory. Polar Biology, 7: 339–343.
- Jager, T., and Ravagnan, E. 2015. Parameterising a generic model for the dynamic energy budget of Antarctic krill *Euphausia superba*. Marine Ecology Progress Series, 519: 115–128.
- Kawaguchi, S., Candy, S. G., King, R., Naganobu, M., and Nicol, S. 2006. Modelling growth of Antarctic krill. I. Growth trends with sex, length, season, and region. Marine Ecology Progress Series, 306: 1–15.
- Kawaguchi, S., Finley, L. A., Jarman, S., Candy, S. G., Ross, R. M., Quetin, L. B., Siegel, V., Trivelpiece, W., Naganobu, M., and Nicol, S. 2007a. Male krill grow fast and die young. Marine Ecology Progress Series, 345: 199–210.
- Kawaguchi, S., Yoshida, T., Finley, L. A., Cramp, P., and Nicol, S. 2007b. The krill maturity cycle: a conceptual model of the seasonal cycle in Antarctic krill. Polar Biology, 30: 689–698.
- Kilada, R., Reiss, C. S., Kawaguchi, S., King, R. A., Matsuda, T., and Ichii, T. 2017. Validation of band counts in eyestalks for the determination of age of Antarctic krill, *Euphausia superba*. PLoS One, 12: e0171773.
- Meyer, B., and Teschke, M. 2016. Physiology of *Euphausia superba*. In Biology and ecology of Antarctic krill. In Advances in polar biology, pp.144–174. Ed. by V. Siegel. Springer, Cham, 441 pp.
- Morris, D. J., Watkins, J. L., Ricketts, C., Buchholz, F., and Priddle, J. 1988. An assessment of the merits of length and weight measurements of Antarctic krill *Euphausia superba*. British Antarctic Survey Bulletin, 79: 27–50.
- Murphy, E. J., Thorpe, S. E., Tarling, G. A., Watkins, J. L., Fielding, S., and Underwood, P. 2017. Restricted regions of enhanced growth of Antarctic krill in the circumpolar Southern Ocean. Nature Scientific Reports, 7: 14.
- Nicol, S., Constable, A. J., and Pauly, T. 2000. Estimates of circumpolar abundance of Antarctic krill based on recent acoustic density measurements. CCAMLR Science, 7: 87–99.
- Nicol, S., de la Mare, W. K., and Stolp, M. 1995. The energetic cost of egg production in Antarctic krill (*Euphausia superba* Dana). Antarctic Science, 7: 25–30.
- Nicol, S., Foster, J., and Kawaguchi, S. 2012. The fishery for Antarctic krill – recent developments. Fish and Fisheries, 13: 30–40.
- Nymand Larson, J., Anisimov, O., Constable, A. J., Hollowed, A., Maynard, N., Prestrud, P., Prowse, T., and Stone, J. 2014. Chapter 28: Polar Regions. In Climate Change 2014: Impacts, Adaptation, and Vulnerability. Report of Working Group II, Vol. 2. Ed. By C. B. Field and R. B. Barros, Intergovernmental Panel on Climate Change, San Francisco, 71 pp.
- Quetin, L. B., and Ross, R. M. 1985. Feeding by Antarctic krill, *Euphausia superba*: does size matter? In Antarctic Nutrient Cycles and Food Webs, pp. 372–377. Ed. by W. R. Siegfried, P. R. Condy, and R. M. Laws. Springer-Verlag Berlin.
- Quetin, L., and Ross, R. 1991. Behavioural and physiological characteristics of the Antarctic krill, *Euphausia superba*. American Zoologist, 31: 49–63.
- R Development Core Team. 2017 R: a language and environment for statistical computing. R Foundation for Statistical Computing, Vienna, Austria. <http://www.R-project.org>.
- Reynolds, R. W., Rayner, N. A., Smith, T. M., Stokes, D. C., and Wang, W. 2002. An improved in situ and satellite SST analysis for climate. Journal of Climate, 15: 1609–1625.
- Rosenberg, A. A., Beddington, J. R., and Basson, M. 1986. Growth and longevity of krill during the first decade of pelagic whaling. Nature, 324: 152–154.
- Rudd, J. T. 1932. On the biology of southern Euphausiidae. Hvalradets Skr, 2: 1–105.
- Ryabov, A. B., de Roos, A. M., Meyer, B., Kawaguchi, S., and Blasius, B. 2017. Competition-induced starvation drives large-scale population cycles in Antarctic krill. Nature Ecology and Evolution, 1: 0177.
- SC-CAMLR. 2002 Annex 4: Working Group on Ecosystem Monitoring and Management. In Report of the Twenty-first Meeting of the Scientific Committee. Commission for the Conservation of Antarctic Marine Living Resources, Hobart, Australia, pp. 123–308.
- SeaWiFS. 2005 Chlorophyll-*a* data: SeaWiFS chlorophyll-*a*. <http://oceancolor.gsfc.nasa.gov/> (last accessed June 2006).
- Siegel, V. 1987. Age and growth of Antarctic Euphausiacea (Crustacea) under natural conditions. Marine Biology, 96: 483–495.
- Siegel, V., and Nicol, S. 2000. Population parameters. In Krill biology, ecology and fisheries. Fish and aquatic resources, vol. 6, pp. 103–149. Ed. by I. Everson. Blackwell Science, Oxford.
- Tarling, G. A., Shreeve, R. S., Hirst, A. G., Atkinson, A., Pond, D. W., Murphy, E. J., and Watkins, J. L. 2006. Natural growth rates in Antarctic krill (*Euphausia superba*): I. Improving methodology and predicting intermoult period. Limnology and Oceanography, 51: 959–972.
- Tarling, G. A., Cuzin-Roudy, J., Thorpe, S. E., Shreeve, R. S., Ward, P., and Murphy, E. J. 2007. Recruitment of Antarctic krill *Euphausia superba* in the South Georgia region: adult fecundity and the fate of larvae. Marine Ecology Progress Series, 331: 161–179.
- Wiedenmann, J., Cresswell, K., and Mangel, M. 2008. Temperature-dependent growth of Antarctic krill: predictions for a changing climate from a cohort model. Marine Ecology Progress Series, 358: 191–202.

Handling editor: Stéphane Plourde